

# Set Up and Test Results for a Vibrating Wire System for Quadrupole Fiducialization

Michael Y. Levashov, Zachary Wolf

August 25, 2006

## Abstract

A vibrating wire system was constructed to fiducialize the quadrupoles between undulator segments in the LCLS. This note studies the ability of the system to fulfill the fiducialization requirements.

## 1 Introduction<sup>1</sup>

Quadrupoles will be placed between the undulator segments in LCLS to keep the electron beam focused as it passes through. The quadrupoles will be assembled with their respective undulator segments prior to being placed into the tunnel. Beam alignment will be used to center the quadrupoles, along with the corresponding undulators, on the beam. If there is any displacement between the undulator and the quadrupole axes in the assemblies, the beam will deviate from the undulator axis. If it deviates by more than  $80\mu m$  in vertical or  $140\mu m$  in horizontal directions, the undulator will not perform as required by LCLS [1]. This error is divided between three sources: undulator axis fiducialization, quadrupole magnetic axis fiducialization, and assembly of the two parts. In particular, it was calculated that the quadrupole needs to be fiducialized to within  $25\mu m$  in both vertical and horizontal directions.

A previous study [2] suggested using a vibrating wire system for finding the magnetic axis of a quadrupole. The study showed that the method has high sensitivity (up to  $1\mu m$ ) and laid out guidelines for constructing it.

---

<sup>1</sup>Work supported in part by the DOE Contract DE-AC02-76SF00515. This work was performed in support of the LCLS project at SLAC.

There are 3 steps in fiducializing the quadrupole with the vibrating wire system. They are positioning the wire at the magnet center (step 1), finding the wire with position detectors (step 2), and finding the quadrupole tooling ball positions relative to the position detector tooling balls (step 3). The following break up of error was suggested for the fiducialization steps:  $10\mu m$  for step 1 (finding the center),  $20\mu m$  for step 2 (finding the wire), and  $10\mu m$  for step 3 (tooling ball measurements).

The purpose of this study is to investigate whether the vibrating wire system meets the requirements for LCLS. In particular, if it can reliably fiducialize a quadrupole magnetic center to within  $25\mu m$  in both vertical and horizontal directions. The behavior of individual system components is compared to the expected performance.

## 2 Setup

A vibrating wire system was constructed as described in [2].

Figure 1 shows photographs of the setup. Although invisible in the pictures, a  $100\mu m$  diameter wire is stretched between two posts (**P1** and **P2** in the figures). The ends of the wire are connected to a function generator (**FG**). A weight (**W**) keeps the wire under a constant tension. The wire goes through a quadrupole magnet (**QM**) that is on top of a supporting stand (**ST**). A motor controller allows the stand to move in  $x$  and  $y$  directions and change pitch and yaw. Note that instead of the quadrupoles that will be used in LCLS, a permanent quadrupole is used, since the electromagnets are not yet available. This, however, should have no effect on the validity of this study.

The wire position is measured by the  $x$  (**PX1** and **PX2**) and  $y$  (**PY1** and **PY2**) position sensors. The signals are amplified (**PA1**, **PA2**, **PA3** and **PA4**) and fed into a voltmeter (**VM**). There is big power line pick up noise in the position detector signal, but it seems to be removed completely by the voltmeter, since it integrates over power line frequency.

A sensor (**VD**) measures the  $x$  and  $y$  components of wire vibration. The signals from the sensor are amplified (**VAX** and **VAY**) and fed into lock-in amplifiers (**LIX** and **LIY**), which are locked on to the function generator signal. At resonance frequency, the wire vibration is  $90^\circ$  out of phase with the generator signal. This allows the relevant signal to be easily picked out from the noise by the lock-ins.

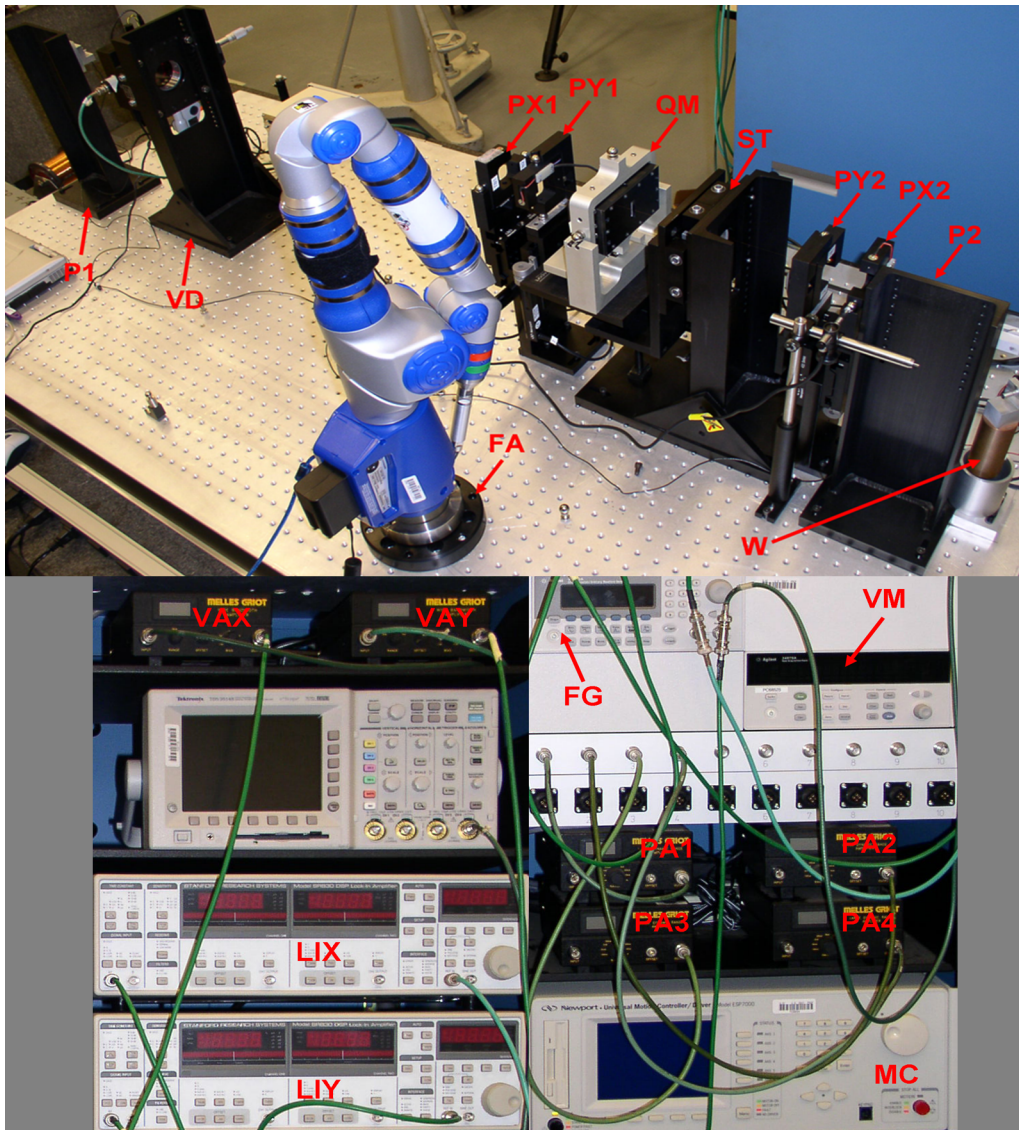


Figure 1: Setup

Finally, a FARO arm (**FA**) is used to measure the position of the tooling balls on the position detectors and the magnet.

### 3 Measurements and Analysis

#### 3.1 Position detector calibration

When the detector is centered on the wire, the distance between the wire and one of its tooling balls is a constant, and can be determined by a calibration. A coordinate measuring machine or a FARO arm can then be used to find the absolute position of the tooling balls on the detectors, allowing the absolute

wire position to be determined.

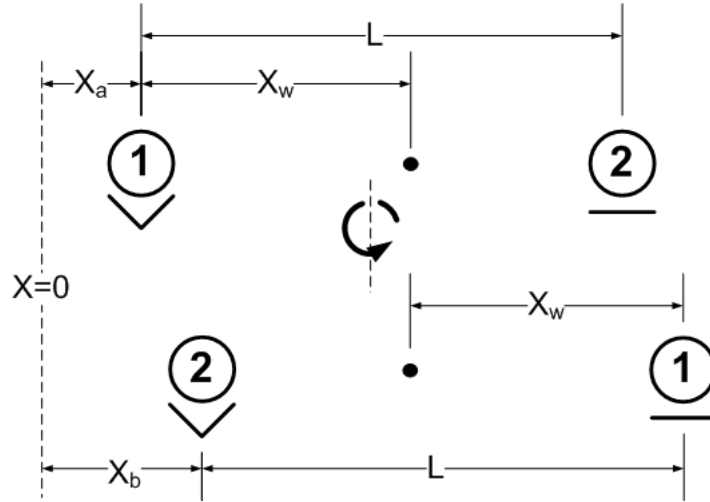


Figure 2: Position Detector Calibration

The top part of the figure shows the original detector position, while the bottom shows the same detector flipped around the vertical axis. The dashed line on the left is an arbitrary origin. The black dot is the wire. Note that the distance between tooling ball **1** and the wire is the same in both cases.

The distances between the tooling balls were measured for all 4 position detectors using a coordinate measuring machine to within  $7\mu m$  or less.

A position detector was placed into its holder and aligned on the wire, giving a scale reading  $x_a$  (Figure 2, top). It was then flipped by  $180^\circ$  such that the tooling ball that was in a vee was now on a flat and vice versa. It was aligned on the wire again, giving a scale reading of  $x_b$  (Figure 2, bottom). The horizontal distance from the wire to tooling ball **1** was calculated as

$$x_w = \frac{L + x_b - x_a}{2} \quad (1)$$

The distance to tooling ball **2** is  $L - x_w$ .

The same procedure was repeated to find  $x_w$  for the other 3 detectors.

The position detectors were found to have a repeatability of  $2\mu m$  for finding the wire. Propagating the errors for the calculation of  $x_w$  gave an uncertainty of  $4\mu m$  or less. Any systematic errors in the measurement of position should be removed by the flipping during calibration.

### 3.2 Position detector check

First, the 4 position detectors were centered on the wire. Next, the positions of the tooling balls of the detectors were found using the FARO arm to approximately  $25\mu m$ . Using the previously found calibration constants, the position of the wire with respect to each of the detector was calculated.

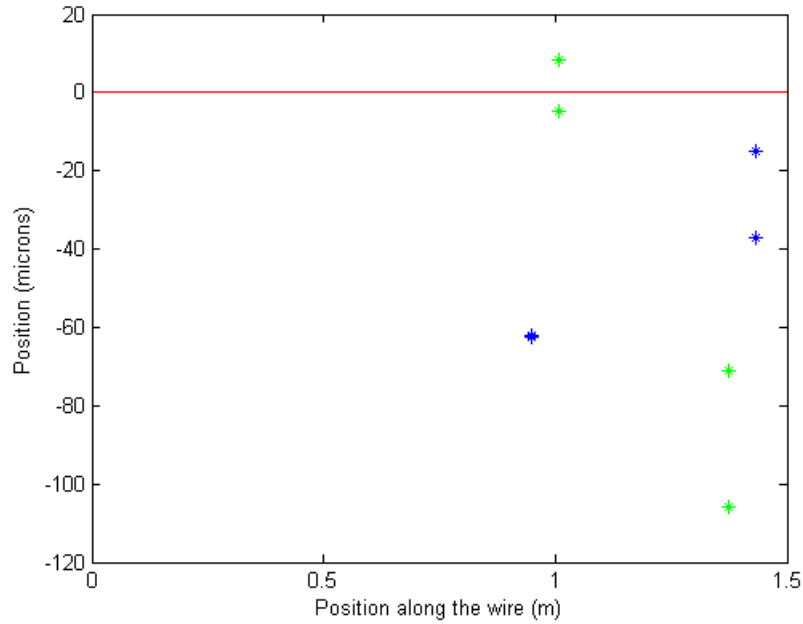


Figure 3: Position Detector Data

The blue points indicate the position of the wire as calculated from the  $x$  position detector tooling balls, with each point corresponding to a tooling ball (the leftmost two points coincide). The green points are the calculated positions from the  $y$  detectors. The red horizontal line at 0 is the actual wire position.

The position of the wire ends were measured using the FARO arm. The wire is under tension, so it will be straight when there are no outside forces acting on it. However, there is gravity acting on the wire. The position detector results were adjusted for the wire sag (explained later in the paper).

The results are shown in Figure 3.

The data for one of the  $y$  detectors (green points in the figure) is close to

the actual wire position. The  $13\mu m$  difference between the two points is due to FARO arm errors plus calibration error.

The data for the second  $y$  detector averages to approximately  $90\mu m$  with a difference of  $35\mu m$  between the two points. This is because the detector tooling balls were hard to access with the FARO arm. A significant force was applied to the tooling balls during the measurement, changing the detector position.

A similar effect may have caused the errors in  $x$  detector data. However, there is  $0\mu m$  difference between the two data points for the first  $x$  detector, but a big offset of  $62\mu m$  for the two, which might mean a bad calibration.

### 3.3 Magnet Flip Test

The quadrupole magnetic center is found by moving the wire until its vibration at the second resonance frequency goes to 0. This means that

$$\int_0^L \vec{B}(z) \sin\left(\frac{2\pi z}{L}\right) dz = 0 \quad (2)$$

when the wire is at the magnet center.

The magnetic field in the equation consists of the field produced by the magnet and any external fields:  $\vec{B} = \vec{B}_m + \vec{B}_{ext}$ .

$$\int_0^L \vec{B}_m(z) \sin\left(\frac{2\pi z}{L}\right) dz = - \int_0^L \vec{B}_{ext}(z) \sin\left(\frac{2\pi z}{L}\right) dz \quad (3)$$

If  $\vec{B}_{ext} \neq 0$ , it is possible for equation 3 to be satisfied when  $\vec{B}_m \neq 0$  and the wire is not at the magnet center.

A uniform field, such as the Earth's, should not be a problem, since its second Fourier component is zero. However, the field may not be perfectly uniform around the setup and there may be other fields present. This will show up as an offset when the magnet is centered on the wire. To check the effect of external fields on the magnet, the following measurements were performed.

#### 3.3.1 X Measurements

Consider a quadrupole sitting on two tooling balls, labeled **1** and **2** for convenience (Figure 4A). The quadrupole is mounted on a support that places a vee under one ball and a flat under the other. The position of the quadrupole

is adjusted until the signal goes to zero, i.e. until equation 2 is satisfied. The wire is now supposed to be located at the quadrupole center, but it may actually be displaced in the  $x$  and  $y$  directions by  $k_x$  and  $k_y$ , respectively. This particular measurement is concerned with  $k_x$ ;  $k_y$  is dealt with in the next section.

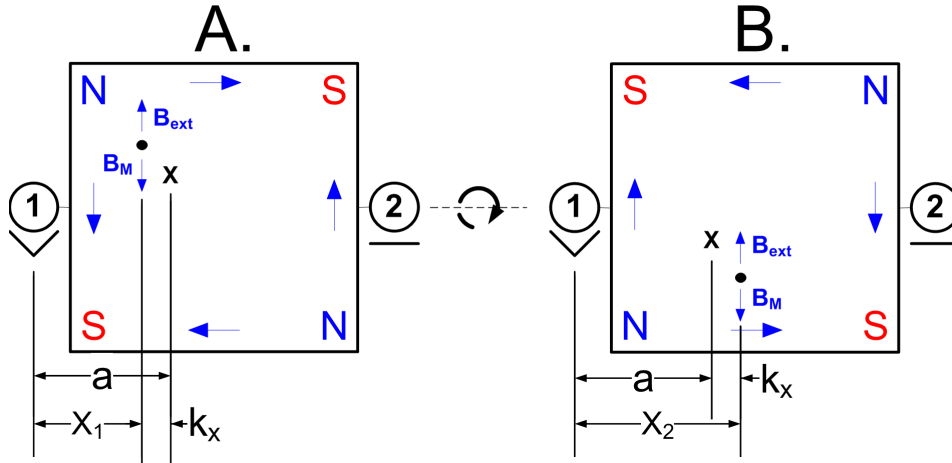


Figure 4: Magnet Flip

Parts A and B of the figure show the magnet before and after it is flipped around the horizontal axis, respectively. Tooling ball **1** is sitting in a ‘vee’ in both cases, while tooling ball **2** is on a flat. The magnetic center of the quadrupole is represented by an  $\mathbf{X}$  symbol. The black dot represents the location of the wire inside the quadrupole at which the wire vibration goes to zero. Only vertical components of  $B_{ext}$  and  $B_m$  are shown.

Let  $x_1$  be the horizontal distance between the present position of the wire and tooling ball **1**. Let  $a$  be the horizontal distance between the quadrupole magnetic center and tooling ball **1**. By definition,  $k_x = a - x_1$ .

The magnet is flipped by rotating it around the horizontal axis by  $180^\circ$ , so tooling balls **1** and **2** stay in the same holders (Figure 4B). When the flip was performed, the magnetic center ( $\mathbf{X}$  in the figure) remained at the same horizontal distance  $a$  from tooling ball **1**. Its vertical position changed, but that is not important for this measurement.

The quadrupole position is adjusted to give zero wire vibration.  $x_2$  is the new horizontal distance between the wire and tooling ball **1** (Figure 4B).

The magnetic field direction around the center has reversed. In order to

get zero wire vibration, equation 3 must be satisfied. The wire remained in the same position, so  $\vec{B}_{ext}$  is the same as before. Therefore, the wire is located such that  $\vec{B}_m$  is also the same as before the flip. Assuming the field magnitude is approximately symmetric around the magnetic center, the wire is displaced by the same  $k_x$  as before, but in the opposite direction. Therefore,  $k_x = x_2 - a$ .

So, the horizontal error in the magnet alignment is

$$k_x = \frac{x_2 - x_1}{2}. \quad (4)$$

$x_2 - x_1$  is how much the magnet has moved between the measurements and was measured by using an indicator.

The wire had to be removed to flip the magnet. That means that the wire could have shifted between the measurements. The wire position detectors were used to find the wire position before and after the magnet was flipped. From this and the indicator measurements,  $x_2 - x_1$  was calculated.

The table below lists results of three such measurements of  $k_x$ .

Point #	$k_x$ ( $\mu m$ )
1	$9 \pm 3$
2	$-1 \pm 2$
3	$-2 \pm 2$
Average	$2 \pm 4$
Variance	6

### 3.3.2 Y Measurements

A similar setup and procedure were used to measure  $k_y$ . This time between the two measurements the quadrupole is rotated around the y axis. Let  $y_1$  and  $y_2$  be the vertical distances between one of the tooling balls and the wire before and after the flip, respectively. Similarly to the X direction,

$$k_y = \frac{y_2 - y_1}{2} \quad (5)$$

and  $k_y$  was calculated by using the results from position detectors and an indicator.



Point #	$k_y$ ( $\mu m$ )
1	$16 \pm 4$
2	$9 \pm 3$
3	$8 \pm 3$
Average	$11 \pm 3$
Variance	4

## 4 Finding the tooling balls

In order to fiducialize the magnet, the location of the magnet tooling balls in relation to the position detector tooling balls needs to be determined.

For this study, we used a FARO arm to measure the location of tooling balls. It provided an accuracy on the order of  $25\mu m$  (in each of 3 coordinates) for locating a tooling ball. This is not satisfactory for LCLS, since it means an error of approximately  $40\mu m$  for the distance between two balls.

A coordinate measuring machine can be used to find distance between tooling balls with accuracy of better than  $10\mu m$ . The machine will have to be used for every quadrupole, unless a way is found to use the machine to calibrate another tool (such as an indicator) for the rest of the measurements.

## 5 Discussion

### 5.1 Finding the Magnetic Center

The first step of the measurement is to align the magnet on the wire. The repeatability of the alignment is  $2\mu m$ .

The shift between the wire and magnet center was small for the  $x$  direction, but was found to be  $11 \pm 3\mu m$  vertically. This means that there are second Fourier components to the external magnetic field in the  $x$  direction.

There were some steel parts (bolts, nuts, mover parts, etc.) near the setup, but only 0.05 Gauss variation of magnetic field along the wire was measured with a flux gate probe. Just in case, the amount of magnetic metals present when fiducializing quadrupoles for LCLS will need to be minimized as much as possible.

Overall, the system performed slightly worse than the  $10\mu m$  suggested in the system requirements.

## 5.2 Finding the Wire

The next step is moving the position detectors on to the wire. The position detectors had a repeatability of  $2\mu m$ . The calibration (finding the distance between the wire and a tooling ball) was done with an uncertainty of  $4\mu m$  or less.

This exceeds the requirements of  $20\mu m$  accuracy for the second fiducialization step.

Note that the magnet flip experiment not only tested how well the magnet center aligns with the wire, but also involved position detector measurements. Therefore, the  $11 \pm 3\mu m$  error mentioned in the previous section is the error in both the first (centering) and second (wire position) steps.

Adding to it the calibration error of the position detectors gives  $11 \pm 5\mu m$ . The required accuracy for the first two steps combined is  $22\mu m$ . Therefore, even though the error in the magnetic center alignment is too large, taken together the two steps are well within the LCLS requirements.

The position detector check can't tell if the calibration of the detectors meets the requirements, because of the high uncertainty in the FARO arm measurements.

## 5.3 Measuring Tooling Balls

The position detector check showed that the whole process of fiducializing the wire position is accurate to at least  $100\mu m$ , when a FARO arm is used. There was big error (up to  $50\mu m$ ) when finding the endpoints of the wire, which might in part account for the poor results.

This is the only step of the measurement that does not meet the LCLS requirements.

Much better results are expected if a coordinate measuring machine is used. However, even with the best machine it might be difficult to get to all tooling balls without putting forces on the position detectors or their stands. A significant force may move the position detector off the wire and a realignment will be necessary. After the tooling balls are measured, the position detectors can be realigned to check that they remained at the same position.

If carefully done with sensitive enough equipment, this step can achieve the LCLS requirement of  $10\mu m$  according to coordinate measuring machine manufacturer specifications.

## 6 Component Performance Analysis

Before the vibrating wire system can be used for LCLS, it is important to make sure that the system is thoroughly understood and all of its components behave as expected.

### 6.1 Resonance Frequency

For a thin wire stretched between two attachment points, the fundamental resonance frequency can be approximated as

$$f_1 = \frac{1}{2L} \sqrt{\frac{T}{m_l}}, \quad (6)$$

where  $L$  is the wire length,  $T$  is the wire tension and  $m_l$  is its mass per unit of length.

It was found that  $L = 1.477m$  and  $T = 9.51N$ , while  $m_l = 6.77 \times 10^{-5} \frac{kg}{m}$  from the manufacturer's specifications, giving an  $f_1 = 127Hz$ . So, the second resonance frequency should be 254Hz. Lower values in the range between 220Hz and 240Hz were usually encountered.

The pins, which are used to guide the wire, have high friction. The calculation above assumed that the wire tension equals the weight on the end, which may not be true.

### 6.2 Wire Sag

The force of gravity produces a sag in the wire in a known direction that can be calculated precisely from the fundamental frequency ( $f_1$ ) as

$$s = \frac{g}{32f_1^2} = 23\mu m, \quad (7)$$

taking the measured fundamental frequency as 115Hz.

When the wire sags it takes the shape of a catenary.  $s$  is the lowest point on it, located at the middle of the wire. From  $s$ , the sag at any other point can be calculated; the table below lists the calculated sag for some important points.

Part	Sag ( $\mu m$ )
PX1	22
PY1	21
PX2	3
PY2	6
Magnet	18

These results were used for the position detector check earlier in the text.

### 6.3 Vibration Detector

Figure 5 shows the response of the  $x$  (left) and  $y$  (right) vibration sensors.

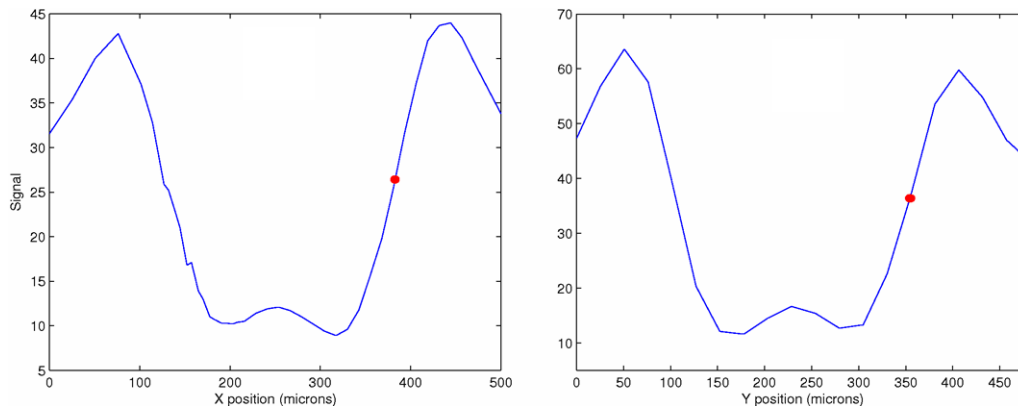


Figure 5: Vibration Detector Response

Vibration detector signals around a  $100\mu m$  wire for  $x$  (left) and  $y$  (right).

Note, that the two plots both have two inclines, each having an approximately constant slope. The detectors were positioned, such that the wire at rest is located approximately in the middle of an incline (red dots in the figures), ensuring a linear response from the sensors.

### 6.4 Position Detector

Figure 6 shows the response of a wire position detector. To find the position of the wire middle, the median signal was determined. The x coordinates at which the median signal occurs were averaged to find the middle of the wire with a repeatability of  $2\mu m$ .

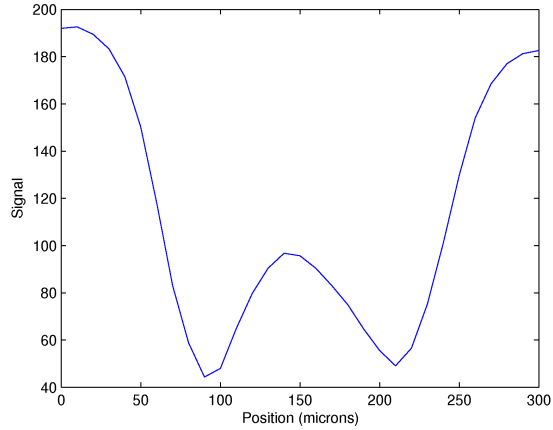


Figure 6: Position Detector Response

Position detector signal around a  $100\mu m$  wire. The response is similar to that of the vibration detectors.

Some asymmetry and strong interference patterns are visible. However, when the detector is flipped, the graph's abscissa also flips, so the asymmetry does not affect the calibration.

## 6.5 Decay constant

To measure the decay constant for wire oscillations, the wire was plucked and the signal from the vibration sensor was read on an oscilloscope. Comparing a few points on the waveform gave an approximation for the time constant.

Try #	$\tau$ (ms)
1	680
2	860
3	620
4	880
5	880
6	640
Average	$760 \pm 50$

A decay constant of  $1s$  was reported in [2]. This is an approximate value. The higher precision result in that study was  $800ms$ , which is consistent with the above data.

## 6.6 Sensitivity

### 6.6.1 Calculated

Formulas for the expected sensitivity of the vibrating wire system to magnet displacements have been previously derived[2].

Equation 8 gives the sensitivity for  $x$  and  $y$  movement.

$$S_{xy} = \frac{I_0 GL_Q}{\sqrt{2\pi m_l f_2 \alpha} L} \quad (8)$$

Equation 9 gives the sensitivity to pitch and yaw.

$$S_{\theta\phi} = \frac{I_0 GL_Q}{3m_l f_4 \alpha} \left( \frac{L_Q}{L} \right)^2 \quad (9)$$

Sensitivity is measured in  $\mu m$  of wire amplitude per  $\mu m$  of displacement for  $x$  and  $y$  shifts and  $\mu m$  of wire amplitude per  $mrad$  of turn for pitch and yaw.

In the equations,  $I_0 = 0.0067A$  is the current amplitude,  $GL_Q = 6.033T$  is the quadrupole integrated gradient,  $m_l = 6.77 \times 10^{-5}kg/m$  is the wire mass per unit length,  $L_Q = 0.033m$  is the quadrupole length,  $L = 1.477m$  is the wire length, and  $\alpha = 2/\tau = 2.6s^{-1}$  is a damping constant.  $f_2 = 230Hz$  and  $f_4 = 460Hz$  are the approximate experimental values for the second and fourth resonance frequencies, respectively.

Plugging in the values gives

$$S_{xy} = 0.15 \pm 0.01\mu m/\mu m \quad (10)$$

$$S_{\theta\phi} = 0.082 \pm 0.008\mu m/mrad \quad (11)$$

### 6.6.2 Experimental

The sensitivities were also determined experimentally. First, the magnet was moved in  $x$  and  $y$ , and rotated around two axes to determine how the lock-in signal depends on the magnet position. The relationships were linear, and slopes for all 4 degrees of freedom were calculated.

When the wire vibrates, it changes position inside the vibration detector around its rest point. The sensitivities of the  $x$  and  $y$  vibration detectors to position changes of the wire were calculated by measuring the slopes in Figures 5-left and 5-right at the wire rest location (indicated by a red point).

The amplification of **VAX** and **VAY** amplifiers was determined with the help of an oscilloscope.

From this data, the wire vibration amplitude per magnet displacement was calculated. The results are summarized in the table below.

Movement Type	Theoretical Sensitivity	Experimental Sensitivity	Units
X	$0.15 \pm 0.01$	$0.16 \pm 0.01$	$\mu m/\mu m$
Y	$0.15 \pm 0.01$	$0.18 \pm 0.01$	$\mu m/\mu m$
Pitch	$0.082 \pm 0.008$	$0.088 \pm 0.005$	$\mu m/mrad$
Yaw	$0.082 \pm 0.008$	$0.081 \pm 0.006$	$\mu m/mrad$

The results are in good agreement. X, Pitch and Yaw sensitivities are all within the calculated uncertainties. The measured Y is 2 standard deviations away, but still close to the calculated value.

## 6.7 Magnet Movement Coupling

If the quadrupole magnetic center was perfectly aligned with the supporting platform, the  $x$ ,  $y$ , pitch, and yaw movements would be independent to second order. However, this was not the case in this study. The movers have coupled directions, mostly pitch and yaw couple to  $y$  and  $x$ , respectively.

To account for the coupling either a smart algorithm can be used or, like in this study, the program can converge on the correct magnet position by repeatedly aligning all of the movement directions. A combination of both will probably be used for the LCLS quadrupoles.

This study showed that even with coupling, the system still repeatably converges on the correct solution. Typically, it took about 3 or 4 iterations to converge. If the magnet is initially placed within  $20\mu m$  from the center for both  $x$  and  $y$ , and within  $10mrad$  for pitch and yaw, the program converges in 2 iterations.

## References

- [1] H. D. Nuhn et al. General undulator system requirements. LCLS Physics Requirements Document 1.4-001, SLAC.
- [2] Z. Wolf. A vibrating wire system for quadrupole fiducialization. LCLS Technical Note LCLS-TN-05-11, SLAC, 2005.